Tetrahedron 68 (2012) 323–328

Contents lists available at SciVerse ScienceDirect

Tetrahedron

journal homepage: www.elsevier.com/locate/tet

Intramolecular homolytic substitution of seleninates – a computational study

Anne C. Neves [a,b,c], Heather M. Aitken [a,b], Sara H. Kyne [a,b], Louis Fensterbank [c], Emmanuel Lacôte [c], Max Malacria [c], Cyril Ollivier [c], Carl H. Schiesser [a,b,*]

[a] ARC Centre of Excellence for Free Radical Chemistry and Biotechnology, Australia
[b] School of Chemistry and Bio21 Molecular Science and Biotechnology Institute, The University of Melbourne, Victoria 3010, Australia
[c] UPMC Université Paris 06, Institut Parisien de Chimie Moléculaire, 4 place Jussieu, C. 229, 75005 Paris, France

ARTICLE INFO

Article history:
Received 12 July 2011
Received in revised form 21 September 2011
Accepted 10 October 2011
Available online 19 October 2011

Keywords:
Radical
Homolytic substitution
Selenium
Seleninates
Computational chemistry

ABSTRACT

Ab initio and density functional theory (DFT) calculations predict that intramolecular homolytic substitution by alkyl radicals at the selenium atom in seleninates proceeds through smooth transition states in which the attacking and leaving radicals adopt a near collinear arrangement. When forming a five-membered ring and the leaving radical is methyl, G3(MP2)-RAD calculations predict that this reaction proceeds with an activation energy ($\Delta E_1^{\ddagger}$) of 30.4 kJ mol^{-1}. ROBHandHLYP/6-311++G(d,p) calculations suggest that the formation of five-membered rings through similar intramolecular homolytic substitution by aryl radicals, with expulsion of phenyl radicals, proceeds with the involvement of a hypervalent intermediate. This intermediate further dissociates to the observed products, with overall energy barriers of about 40 kJ mol^{-1}. Homolytic addition to the phenyl group was found not to be competitive with substitution, with a calculated barrier of 57.6 kJ mol^{-1}. This computational study provides insight into homolytic substitution chemistry involving seleninates.

1. Introduction

Intramolecular homolytic substitution chemistry provides an effective method for the preparation of sulfur-containing heterocycles.[1–4] While examples can be found of alkyl, aryl, and acyl radicals undergoing this chemistry at the sulfur atom in sulfides,[2–4] sulfoxides,[5–9] sulfinates,[10,11] and sulfinamides,[10,11] to the best of our knowledge there are no examples reported for this chemistry involving sulfones.[7–9] The examples depicted in Scheme 1 illustrate the versatility of this chemistry; radicals derived from acylselenides (e.g., **1**), aryl and alkyl bromides (e.g. **2**, **3**) afford thiolactones,[12] cyclic sulfoxides,[5] and sultines[10,11] in good yield.

While the majority of intramolecular radical substitution chemistry has involved attack at sulfur, there are also numerous examples of the formation of selenium and tellurium containing rings using these reactions, some of which are displayed in Scheme 2. Diazonium salts, such as **4** are effectively converted into the corresponding aryl radical that undergoes sequential addition to ethyl propiolate followed by intramolecular substitution at selenium to afford the benzoselenophene,[13] while epoxide **5** reacts with sodium butyltelluroate to give the dihydrobenzotellurophene in a process involving aryl radical attack at tellurium.[14,15]

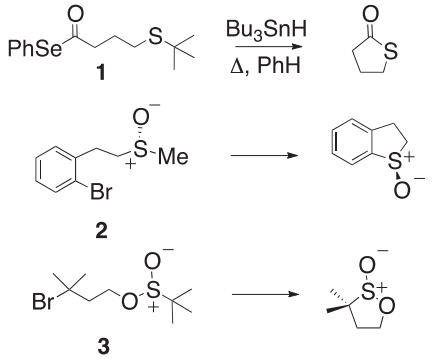

Scheme 1.

It is interesting to note that there appear to be no examples of ring formation reactions involving homolytic substitution at oxidized selenium or tellurium.

Recently, we showed that cyclic sulfinates and sulfonamides could be prepared utilizing this chemistry,[10,11] and more recently that computational chemistry provided valuable insight into the intimate mechanistic details of the key bond-forming and bond-breaking steps.[16]

With an inherent interest in homolytic substitution reactions involving selenium and their further development,[17] we chose

* Corresponding author. Tel.: +61 3 8344 2432; fax: +61 3 9347 8189; e-mail address: carlhs@unimelb.edu.au (C.H. Schiesser).

0040-4020/$ – see front matter © 2011 Elsevier Ltd. All rights reserved.
doi:10.1016/j.tet.2011.10.037

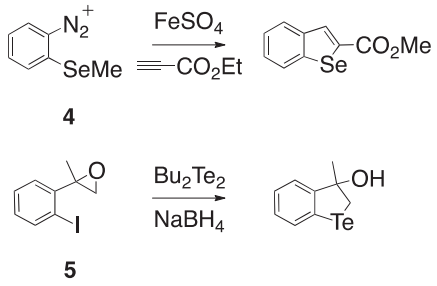

Scheme 2.

to explore the analogous intramolecular homolytic chemistry involving seleninates. We now report that intramolecular homolytic substitution by alkyl and aryl radicals at the selenium atom in seleninates with the expulsion of alkyl radicals proceeds through a transition state in which the attacking and leaving radicals adopt a near collinear arrangement. Similar chemistry involving aryl radicals with a phenyl leaving group is calculated to take place with the involvement of a hypervalent intermediate.

2. Computational methods

Ab initio and density functional theory (DFT) calculations were carried using the Gaussian 09 program.[18] Geometry optimizations were performed with standard gradient techniques at HF, MP2, BHandHLYP, M05-2X and M06-2X levels of theory, using restricted methods for closed-shell systems.[19] Many DFT methods, including B3LYP, perform poorly for radical systems,[20] and this is often associated with an inadequate treatment of exchange terms.[21] Zipse showed some time ago that, as a DFT method, BHandHLYP provides a good compromise,[22] and we reported that this method often provides data that reflect those obtained using higher correlation methods, such as QCISD or CCSD(T).[23–25]

All ground and transition states in this study were verified by vibrational frequency analysis. As was apparent in our earlier study involving sulfinates,[16] spin contamination proved to be a significant problem for some open-shell systems, especially for transition states and hypervalent intermediates, with UHF, UMP2 and UBHandHLYP methods providing values of $\langle s^2 \rangle$ often in excess of 2 before annihilation of quartet contamination; UQCISD and UCCSD(T) were much better behaved. As a result, all optimizations of open-shell molecules were carried out using restricted open-shell methods (ROHF, ROBHandHLYP). Standard basis sets available in Gaussian 09 were used. Improved energies were then obtained on selected structures as detailed in Table 1 through single-point (ROMP2, QCISD, CCSD(T)) calculations, and using G3(MP2)-RAD,[26] a high-level composite method that approximates (U)RCCSD(T) calculations with a large triple-ζ basis set via additivity corrections at the ROMP2 level of theory. G3(MP2)-RAD has been shown to reproduce a large test set of experimental data to within chemical accuracy.[26] Zero-point vibrational energy (ZPE) corrections have been applied to all optimized structures.

Optimized geometries and energies for structures **7**, **9**–**13** (Gaussian Archive entries) are available as Electronic Supplementary data.

3. Results and discussion

3.1. Ring closure of radical 6 (R=Me)

We began this work by examining the potential energy surface for the cyclization of the 'parent' reaction (R=Me) depicted in Scheme 3. This study aimed to provide a comparison with the analogous 'parent' sulfinate system,[16] while at the same time affording valuable benchmarking data and confidence in the computational methods used.

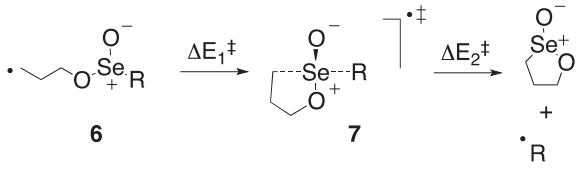

Scheme 3.

Searching of the $C_4H_9O_2Se$ potential energy surface located structures **6** and **7** (R=Me) as well as the cyclized seleninate and methyl radical. Structure **6** (R=Me) proved to correspond to an energy minimum as verified by vibrational frequency analysis, while **7** (R=Me) proved to be a transition state; structure **7** is displayed in Fig. 1, while important geometrical features of **7** at each optimized level of theory are listed in Table 1 together with pertinent energy data.

Inspection of Fig. 1 reveals that transition state **7** (R=Me), with BHandHLYP/6-311++G(d,p) calculated key distances of 2.066 and 2.212 Å, like its sulfur counterpart,[16] is 'late' in the direction of reaction depicted in Scheme 3. Similar data are provided at the other levels of theory employed in this study (Table 1); indeed there appears to be little variation in r_1 and r_2 with theoretical level.

Table 1
Calculated activation energies ($\Delta E_1^{\ddagger}$, $\Delta E_2^{\ddagger}$) for the cyclization of radical **6** (R=Me, Scheme 3), and key data for transition structure **7** (R=Me)

Level of theory	$\Delta E_1^{\ddagger}$[a]	$\Delta E_1^{\ddagger}$+ZPE[a]	$\Delta E_2^{\ddagger}$	$\Delta E_2^{\ddagger}$+ZPE[a]	r_1[b]	r_1[b]	ν_{TS}[c]
ROHF/6-31G(d)	109.7	115.7	85.1	100.5	2.067	2.118	499i
ROHF/6-311G(d,p)	122.1	128.2	103.6	120.2	2.064	2.122	502i
ROBHandHLYP/6-311G(d,p)	57.7	62.8	33.9	46.1	2.069	2.210	341i
ROBHandHLYP/6-311++G(d,p)	58.3	63.4	37.1	49.2	2.066	2.212	341i
ROBHandHLYP/cc-pVDZ	60.5	65.2	33.1	45.2	2.076	2.205	345i
ROBHandHLYP/aug-cc-pVDZ	57.5	62.3	36.7	48.2	2.070	2.207	340i
M05-2X/6-311++G(d,p)	28.4	33.1	4.0	14.8	2.076	2.265	262i
M06-2X/6-311++G(d,p)	35.2	39.4	8.6	19.9	2.048	2.326	285i
ROMP2/6-311++G(d,p)//ROBHandHLYP/6-311++G(d,p)	28.0		17.3				
QCISD/6-311++G(d,p)//ROBHandHLYP/6-311++G(d,p)	45.6		30.2				
QCISD/cc-pVTZ//ROBHandHLYP/6-311++G(d,p)	42.1		24.2				
CCSD(T)/6-311++G(d,p)//ROBHandHLYP/6–311++G(d,p)	36.1		21.9				
G3(MP2)-RAD	30.4		22.2				

[a] Energies in kJ mol^{-1}.
[b] Key transition structure separations in Å (see Fig. 1).
[c] Transition state vector (imaginary) frequency.

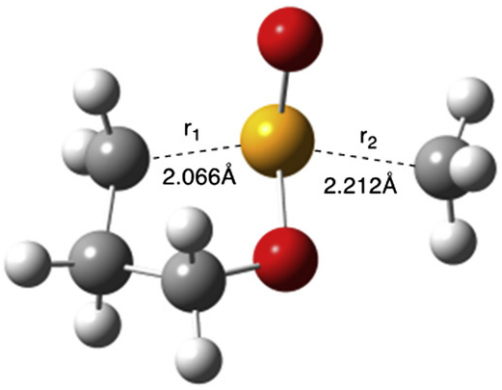

Fig. 1. ROBHandHLYP/6-311++G(d,p) optimized structure of transition state **7** (R=Me). Data at other levels of theory are listed in Table 1.

It is instructive to compare these data with those calculated for other homolytic substitution reactions involving selenium; C–Se transition state separations of 2.0–2.3 Å (depending on level of theory) have been calculated for both inter- and intramolecular reactions involving alkyl radicals at unoxidized selenium.[23,27–29] It is interesting to note that the 'attack angle' in **7** is calculated to be 164° at this level of theory, slightly larger than the 'ideal angle' of about 154° calculated using MP2/DZP for the degenerate reaction of methyl radical with methaneselenol.[28]

The geometrical 'lateness' of transition state **7** (R=Me) is consistent with the energy data provided in Table 1; at all levels of theory the ring closure of radical **6** is calculated to be endothermic. In addition, inclusion of electron correlation also appears to be important in arriving at satisfactory energy barriers. For example, ROHF/6-311G(d,p) calculations provide a value of $\Delta E_1^{\ddagger}$ of 122.1 kJ mol^{-1}, while the barrier for the reverse reaction ($\Delta E_2^{\ddagger}$) is calculated to be 114.6 kJ mol^{-1}; both barriers increase slightly upon inclusion of zero-point vibrational energy (ZPE) correction. Both energy barriers are dramatically lower using DFT, with ROBHandHLYP/6-311++G(d,p) providing values of 58.3 and 41.9 kJ mol^{-1} for $\Delta E_1^{\ddagger}$ and $\Delta E_2^{\ddagger}$, respectively. It is interesting to note that both QCISD methods employed provide values of $\Delta E_1^{\ddagger}$ in the mid-forties (kJ mol^{-1}), while the CCSD(T)/6-311++G(d,p) single-point calculation provides values of 36.1 and 22.0 kJ mol^{-1} for the forward and reverse barriers.

It is also interesting to note the while the M05-2X and M06-2X methods provide values for the 'forward' energy barrier, $\Delta E_1^{\ddagger}$, of 33.1 and 39.4 kJ mol^{-1} that resemble those from the QCISD and CCSD(T) calculations, these methods appear to significantly underestimate $\Delta E_2^{\ddagger}$, providing values of 4.0 and 8.6 kJ mol^{-1}, respectively.

It is clear from the data in Table 1 that the energy barriers at the various levels of theory employed in this study appear to converge to the G3(MP2)-RAD values of about 30 and 22 kJ mol^{-1}, with ROMP2/6-311++G(d,p), on this occasion, giving values close to those provided by the highest level of theory (28.0, 17.4 kJ mol^{-1}). It has been suggested previously that ROMP2 calculations are capable of providing reliable data for a variety of radical reactions,[30] however, this was not generally observed in our previous work involving sulfinates.[16]

It is important to compare the energy data in Table 1 with those of the analogous reaction involving sulfur in which G3(MP2)-RAD calculations provided values of $\Delta E_1^{\ddagger}$ and $\Delta E_2^{\ddagger}$ of 43.2 and 24.4 kJ mol^{-1}.[16] Clearly, as has been observed in other systems, intramolecular homolytic substitution at the selenium atom in a seleninate is predicted to be more facile (by about 13 kJ mol^{-1} for **6**, R=Me) over the analogous reaction at the sulfur atom in a sulfinate.

Unfortunately, QCISD, CCSD(T) and G3(MP2)-RAD methods are not suitable for the remaining systems of interest in this study because of resource limitations. Despite this, and with the knowledge that BHandHLYP methods are likely to overestimate the energy barriers ($\Delta E_1^{\ddagger}$ and $\Delta E_2^{\ddagger}$) by 20–30 kJ mol^{-1}, we chose to continue this study using the above-mentioned DFT method because of the useful qualitative insight that these calculations will provide for a hitherto unknown reaction, namely homolytic substitution at seleninates.

3.2. Effect of leaving group in radical 6 (R=Et, *i*-Pr, *t*-Bu)

We next turned our attention to the effect of the leaving group on the chemistry depicted in Scheme 3. Ground and transition states (**6**, **7**) as well as products were located on the respective potential energy surface for reactions involving primary, secondary and tertiary leaving groups exemplified by R=Et, *i*-Pr and *t*-Bu, and these structures verified as corresponding to the appropriate stationary point by vibrational frequency analysis. Fig. 2 depicts the BHandHLYP/6-311++G(d,p) calculated transition structures **7**, while Table 2 lists calculated energy and geometry data using this level of theory; data obtained at other levels of theory can be found in the Supplementary data.

Inspection of Fig. 2 reveals transition state separations consistent with those calculated for other reactions at selenium (vide

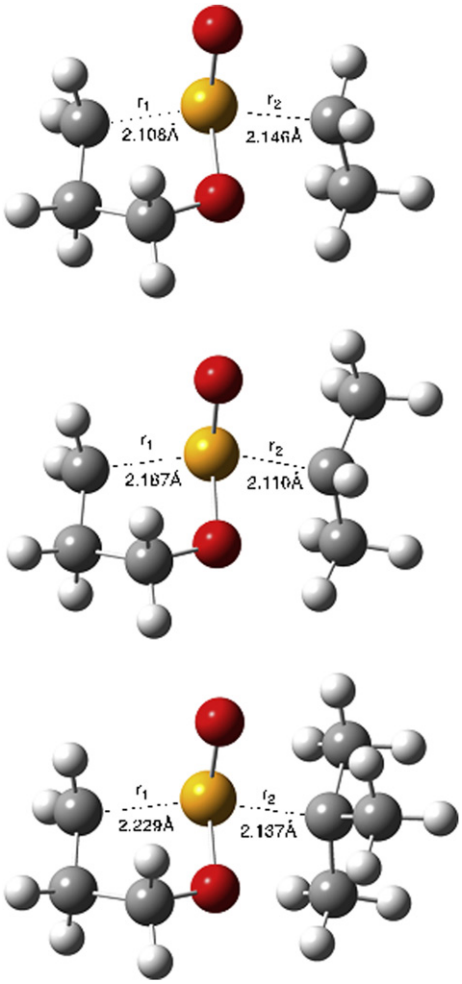

Fig. 2. ROBHandHLYP/6-311++G(d,p) optimized structures of transition states **7** (R=Et, *i*-Pr, *t*-Bu). Data at other levels of theory can be found as Supplementary data.

Table 2
ROBHandHLYP/6-311++G(d,p) calculated activation energies ($\Delta E_1^{\ddagger}$, $\Delta E_2^{\ddagger}$) for the cyclization of radicals **6** (R=Et, *i*-Pr, *t*-Bu, Scheme 3), and associated transition state vector (imaginary) frequency for transition states **7**

Leaving radical (R•)	$\Delta E_1^{\ddagger}$[a]	$\Delta E_1^{\ddagger}$+ZPE[a]	$\Delta E_2^{\ddagger}$[a]	$\Delta E_2^{\ddagger}$+ZPE[a]	ν_{TS}[b]
Ethyl (Et)	51.6	57.8	38.6	49.1	271i
iso-Propyl (*i*-Pr)	44.6	50.6	46.6	55.9	314i
tert-Butyl (*t*-Bu)	42.0	47.6	54.7	60.9	384i

[a] Energies in kJ mol^{-1}.
[b] Transition state vector (imaginary) frequency.

supra) and show that as the leaving group is 'improved' in moving from methyl (Fig. 1) to ethyl, *iso*-propyl and *tert*-butyl, that the reaction becomes 'earlier' in the direction indicated in Scheme 3. This observation is consistent with expectation and with the energy data provided in Table 2 that show progressively lower values for $\Delta E_1^{\ddagger}$ (54.1–42.0 kJ mol^{-1}) in moving through this series. Importantly, this reaction is calculated to be exothermic by about 12 kJ mol^{-1} when *tert*-butyl is used as the leaving radical.

3.3. Ring closure of aryl radicals 8

The substitution chemistry involving aryl radicals **8** was next examined and the reaction profile proved to be highly dependent on the nature of the leaving group (Scheme 4). With alkyl leaving groups (R=Me, *t*-Bu) the reaction profile resembled those of the other reactions studied so far and transition states **9** that connected the starting radicals **8** directly to the products were located. However, when the leaving group was replaced with the phenyl radical, an intermediate (**11**) was located on the $C_{13}H_{11}O_2Se$ potential energy surface, in a similar manner to that previously observed for the corresponding sulfinate.[16]

Fig. 3 depicts the ROBHandHLYP/6-311++G(d,p) calculated transition states **9** (R=Me, *t*-Bu) and reveals that these structures, with calculated values of 2.293 Å (Me) and 2.358 Å (*t*-Bu) for r_1, are 'earlier' than the analogous structures **7** located for alkyl radical attack. This is consistent with the intrinsic reactivity of the aryl radical in comparison with primary alkyl and is also reflected in the energy data shown in Scheme 4; at this level of theory $\Delta E_1^{\ddagger}$ is calculated to be 8–13 kJ mol^{-1} lower than that for the analogous reactions involving **6** (R=Me, *t*-Bu). Data at other levels of theory are provided in the Supplementary data.

Fig. 4 displays the ROBHandHLYP/6-311++G(d,p) calculated structures **10**–**13** predicted to be involved in the radical chemistry of **8** (R=Ph), as well as the associated energy data. As was predicted for the analogous sulfinate,[16] intramolecular homolytic substitution involving **8** (R=Ph) is predicted to proceed with the

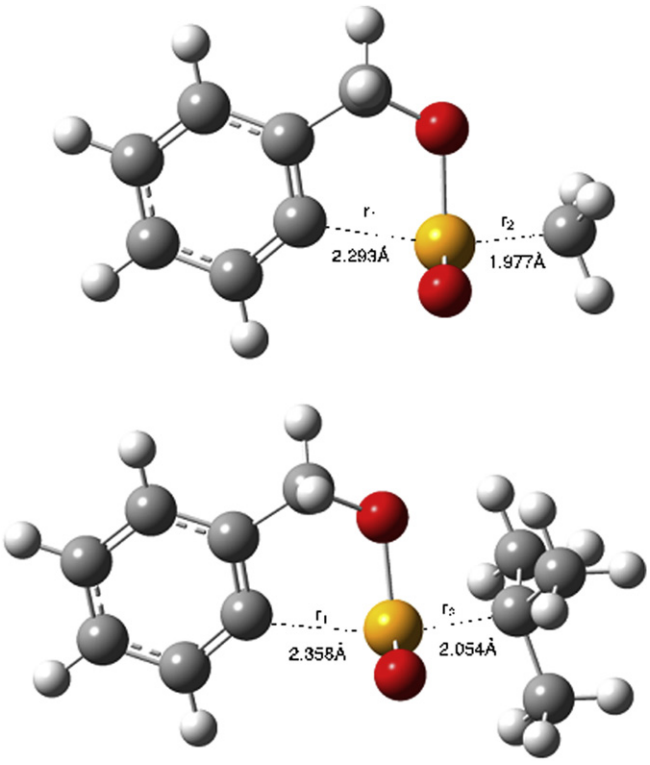

Fig. 3. ROBHandHLYP/6-311++G(d,p) optimized structures of transition states **9** (R=Me, *t*-Bu). Data at other levels of theory can be found as Supplementary data.

involvement of intermediate **11**, which is calculated to lie at some 35.6 kJ mol^{-1} above the starting radical **8** on the potential energy surface. This intermediate lies in a shallow well, with barriers ($\Delta E_2^{\ddagger}$, $\Delta E_3^{\ddagger}$) of about 4 kJ mol^{-1} for dissociation to the starting material, or to the product. At some levels of theory this well effectively disappears when ZPE correction is applied (Table S3; Supplementary data). This activation energy is to be compared with the value of 46.3 kJ mol^{-1} obtained for the corresponding sulfinate.[16] Consequently we predict that the cyclization of **8** (R=Ph) should be more facile than cyclization of the corresponding sulfinate. In competition is intramolecular addition to the aryl 'leaving group' to afford adduct radical **14** via transition state **13**. This process is calculated to require 57.6 kJ mol^{-1} and should not be competitive with the homolytic substitution channel, unlike the corresponding sulfinate.[16]

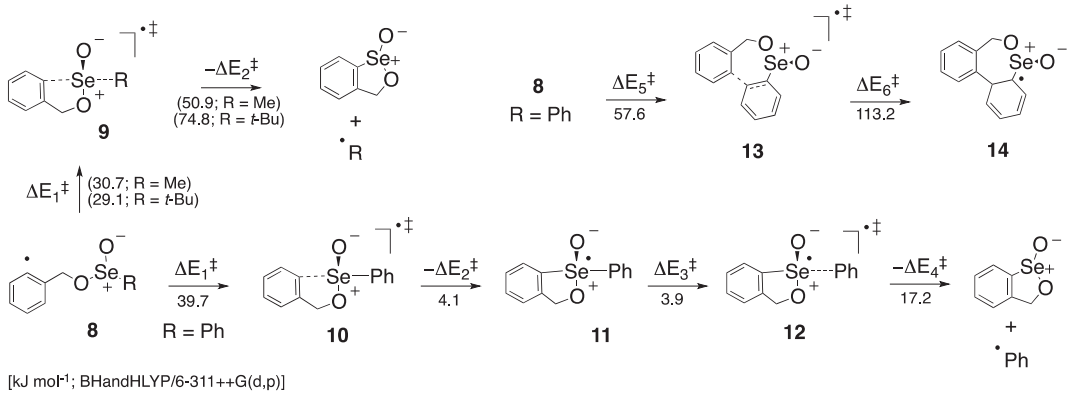

Scheme 4.

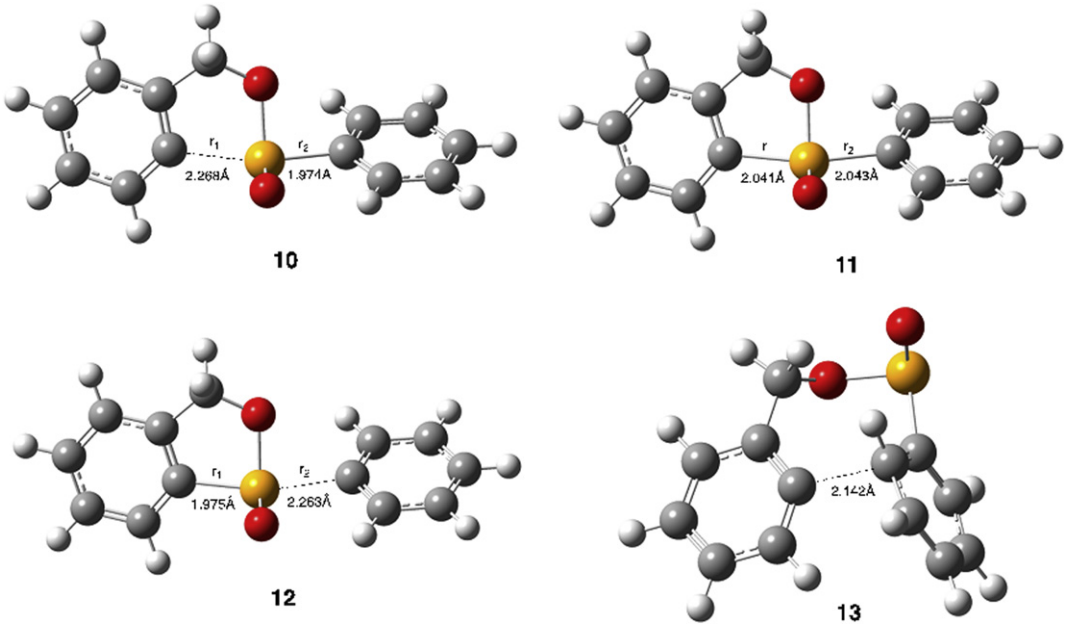

Fig. 4. ROBHandHLYP/6-311++G(d,p) optimized structures of transition states **10**–**13**. Data at other levels of theory can be found as Supplementary data.

4. Conclusion

Ab initio and density functional theory (DFT) calculations predict that intramolecular homolytic substitution by alkyl radicals at the selenium atom in seleninates proceeds through a smooth transition state in which the attacking and leaving radicals adopt a near collinear arrangement. When forming a five-membered ring and when the leaving radical is methyl, G3(MP2)-RAD/calculations predict that this reaction proceeds with an activation energy ($\Delta E_1^{\ddagger}$) of 30.4 kJ mol^{-1}, up to 30 kJ mol^{-1} lower than that calculated using ROBHandHLYP methods. Despite this, ROBHandHLYP/6-311++G(d,p) is able to satisfactorily reproduce the qualitative features observed at the higher levels (G3, CCSD(T)) of theory and has been used to explore the chemistry of the larger systems in this study.

ROBHandHLYP/6-311++G(d,p) calculations suggest that the formation of five-membered rings through intramolecular homolytic substitution by aryl radicals at the selenium atom in seleninates, with expulsion of phenyl radicals, proceeds with the involvement of a hypervalent intermediate. This intermediate further dissociate to the observed products, with an overall energy barrier of about 40 kJ mol^{-1}. This computational study provides insight into the synthetic potential of seleninates in homolytic substitution chemistry.

Acknowledgements

Generous support of the Australian Research Council through the Centres of Excellence Program is gratefully acknowledged. We thank the National Facility of the Australian National Computational Infrastructure and the Victorian Life Sciences Computation Initiative (VLSCI) for generous allocations of computing resources. We also thank UPMC, CNRS, IUF (L.F. and M.M.) and the Master de Chimie for financial support.

Supplementary data

The following are available as Supplementary data: Tables S1–S4; optimized geometries (Gaussian archive entries) of structures **7**, **9**–**13** at all optimized levels of theory used in this study. Supplementary data associated with this article can be found, in the online version, at doi:10.1016/j.tet.2011.10.037.

References and notes

1. Kyne, S. H.; Schiesser, C. H., In *Handbook of Radical Chemistry and Biology*, Chatgilialoglu, C.; Studer, A., Eds.; Wiley: Chichester, UK, in press.
2. Schiesser, C. H.; Wild, L. M. *Tetrahedron* **1996**, *52*, 13265.
3. Walton, J. C. *Acc. Chem. Res.* **1998**, *31*, 99.
4. Crich, D. *Helv. Chim. Acta* **2006**, *89*, 2167.
5. Beckwith, A. L. J.; Boate, D. R. *J. Chem. Soc., Chem. Commun.* **1986**, 189.
6. Kampmeier, J. A.; Jordan, R. B.; Liu, M. S.; Yamanaka, H.; Bishop, D. J., In *Organic Free Radicals*; Pryor, W. A., Ed., ACS Symposium Series No. 69; American Chemical Society: Washington, **1978**.
7. Tada, M.; Nakagiri, H. *Tetrahedron Lett.* **1992**, *33*, 6657.
8. Ooi, T.; Furuya, M.; Sakai, D.; Maruoka, K. *Adv. Synth. Catal.* **2001**, *343*, 166.
9. Crich, D.; Hutton, T. K.; Ranganathan, K. *J. Org. Chem.* **2005**, *70*, 7672.
10. Coulomb, J.; Certal, V.; Fensterbank, L.; Lacôte, E.; Malacria, M. *Angew. Chem., Int. Ed.* **2006**, *45*, 633.
11. Coulomb, J.; Certal, V.; Larraufie, M.-H.; Ollivier, C.; Corbet, J.-P.; Mignani, L.; Fensterbank, E.; Lacôte, E.; Malacria, M. *Chem.—Eur. J.* **2009**, *15*, 10255.
12. Ryu, I.; Okuda, T.; Nagahara, K.; Kambe, N.; Komatsu, M.; Sonoda, N. *J. Org. Chem.* **1997**, *62*, 7550.
13. Lyons, J. E.; Schiesser, C. H.; Sutej, K. *J. Org. Chem.* **1993**, *46*, 1437.
14. Laws, M. J.; Schiesser, C. H. *Tetrahedron Lett.* **1997**, *38*, 8429.
15. Engman, L.; Laws, M. J.; Malmström, J.; Schiesser, C. H.; Zugaro, L. M. *J. Org. Chem.* **1999**, *64*, 6764.
16. Kyne, S. H.; Aitken, H. M.; Schiesser, C. H.; Lacôte, E.; Malacria, M.; Ollivier, C.; Fensterbank, L. *Org. Biomol. Chem.* **2011**, *9*, 3331.
17. Schiesser, C. H. *Chem. Commun.* **2006**, 4055.
18. Frisch, M. J.; Trucks, G. W.; Schlegel, H. B.; Scuseria, G. E.; Robb, M. A.; Cheeseman, J. R.; Scalmani, G.; Barone, V.; Mennucci, B.; Petersson, G. A.; Nakatsuji, H.; Caricato, M.; Li, X.; Hratchian, H. P.; Izmaylov, A. F.; Bloino, J.; Zheng, G.; Sonnenberg, J. L.; Hada, M.; Ehara, M.; Toyota, K.; Fukuda, R.; Hasegawa, J.; Ishida, M.; Nakajima, T.; Honda, Y.; Kitao, O.; Nakai, H.; Vreven, T.; Montgomery, J. A., Jr.; Peralta, J. E.; Ogliaro, F.; Bearpark, M.; Heyd, J. J.; Brothers, E.; Kudin, K. N.; Staroverov, V. N.; Kobayashi, R.; Normand, J.; Raghavachari, K.; Rendell, A.; Burant, J. C.; Iyengar, S. S.; Tomasi, J.; Cossi, M.; Rega, N.; Millam, N. J.; Klene, M.; Knox, J. E.; Cross, J. B.; Bakken, V.; Adamo, C.; Jaramillo, J.; Gomperts, R.; Stratmann, R. E.; Yazyev, O.; Austin, A. J.; Cammi, R.; Pomelli, C.; Ochterski, J. W.; Martin, R. L.; Morokuma, K.; Zakrzewski, V. G.; Voth, G. A.; Salvador, P.; Dannenberg, J. J.; Dapprich, S.; Daniels, A. D.; Farkas, Ö; Foresman, J. B.; Ortiz, J. V.; Cioslowski, J.; Fox, D. J. *Gaussian 09, Revision A.1*; Gaussian: Wallingford CT, 2009.
19. Hehre, W. J.; Radom, L.; Schleyer, P. v. R.; Pople, J. A. *Ab Initio Molecular Orbital Theory*; Wiley: New York, NY, 1986.
20. For example see: Morihovitis, T.; Schiesser, C. H.; Skidmore, M. A. *J. Chem. Soc., Perkin Trans. 2* **1999**, 2041.
21. Tschinke, V.; Ziegler, T. *Theor. Chim. Acta* **1991**, *81*, 65.
22. Mohr, M.; Zipse, H.; Marx, D.; Parrinello, M. *J. Phys. Chem. A* **1997**, *101*, 8942.
23. Horvat, S. M.; Schiesser, C. H. *New J. Chem.* **2010**, *34*, 1692.

24. Kyne, S. H.; Schiesser, C. H.; Matsubara, H. *J. Org. Chem.* **2008**, *73*, 427.
25. Matsubara, H.; Falzon, C. T.; Ryu, I.; Schiesser, C. H. *Org. Biomol. Chem.* **2006**, *4*, 1920.
26. Henry, D. J.; Sullivan, M. B.; Radom, L. *J. Phys. Chem.* **2003**, *118*, 4849.
27. Lyons, J. E.; Schiesser, C. H. *J. Organomet. Chem.* **1992**, *437*, 165.
28. Schiesser, C. H.; Smart, B. A. *Tetrahedron* **1995**, *51*, 6051.
29. Schiesser, C. H.; Wild, L. M. *J. Org. Chem.* **1999**, *64*, 1131.
30. Gomez-Balderas, R.; Coote, M. L.; Henry, D. J.; Radom, L. *J. Phys. Chem. A* **2004**, *108*, 2874.